2-PYRIDINAMINE COMPOSITIONS AND RELATED METHODS

Cross Reference to Related Application

This application claims priority from United States provisional application Serial No. 60/223,795, filed August 8, 2000, which is hereby incorporated by reference.

Field of the Invention

The present invention relates to neuroprotective 2-pyridinamine compositions, and methods of using same to prevent cell death after an ischemic event. The instant compositions have particular importance in preventing neuronal cell death and its resulting disorders.

Background of the Invention

Glutamate is the major fast excitatory neurotransmitter in the mammalian central nervous system. It depolarizes neurons by opening three classes of ligand-gated ion channels: AMPA, kainate, and NMDA receptors. Transient increases in synaptic glutamate levels occur during normal excitatory transmission. However, excessive increases in synaptic glutamate levels are toxic to neurons, and trigger the process of neuronal cell death commonly referred to as glutamate excitotoxicity (Meldrum and Garthwaite 1990). Glutamate excitotoxicity contributes to ischemia-induced brain damage, epilepsy, and various chronic neurodegenerative diseases (Meldrum and Garthwaite 1990).

Of the three classes of glutamate-gated channels, specific overactivation of the N-methyl-D-aspartate (NMDA) receptor is primarily responsible for triggering excitotoxic neuron death in a variety of neuron types (Meldrum and Garthwaite 1990). In animal stroke models, ischemia-induced brain damage can be largely alleviated by pretreatment with the specific NMDA receptor antagonist, MK-801 (Park et al. 1988). In many types of neurons, glutamate exictotoxicity is thought to result primarily from excessive influx of calcium ions due to the high permeability of the NMDA receptor for calcium (Schneggenburger et al. 1993). High intracellular calcium levels may lead to overactivation of calcium-regulated enzymes such as nitric oxide synthase,

phospholipases, proteases and kinases. Further, higgh intracellular calcium levels may mediate excitotoxicity.

Glutamate signaling through the NMDA receptor induces phosphorylation and activation of mitogen-activated protein kinases (MAPK) in primary neuronal cultures (Bading and Greenberg 1991; Xia et al. 1995). Animal models of ischemic brain injury suggest that increased activity of MAPK family members may mediate neuronal injury (Alessandrini et al. 1999; Yang et al. 1997). Deletion of Jnk3, a member of the JNK family of MAP kinases which is predominantly expressed in brain, protects hippocampal neurons from kainic acid-induced excitotoxicity *in vivo*, although the role of the NMDA receptor in this form of toxicity is not clear (Yang et al. 1998). Specific inhibition of the upstream activating kinases of ERK1/2, (p44/42) MAP kinase, protects against neuronal damage due to focal cerebral ischemia (Alessandrini et al. 1999). In cultured primary hippocampal neurons, inhibition of the ERK1/2 (p44/42 MAPK) signaling pathway protects against neuron death induced by removal of kynurenate, a broad spectrum glutamate-receptor antagonist (Murray et al. 1998). Non-receptor-mediated glutamate-induced oxidative toxicity is also blocked by inhibition of the ERK1/2 signaling pathway (Stanciu et al. 2000). Collectively, these reports clearly indicate an important role for ERK1/2 MAPK signaling in glutamate-induced neuronal toxicity. However, it remains unclear as to what class of glutamate receptor can trigger the excitotoxic signaling cascade in which the ERK1/2 MAPK pathway is so critically involved.

Substantial evidence from the literature suggests that MEK (MAP Kinase or ERK Kinase, a threonine-tyrosine kinase activator of ERK1 and ERK2) inhibition is an effective neuroprotective strategy *in vivo* (Alessandrini et al. 1999; Hu and Wieloch 1994; Kindy 1993). These reports indicate that transient cerebral ischemia induces p42 MAP kinase phosphorylation in rodent brain. A selective inhibitor of MEK1/2, PD 098059, can block this induction in phosphorylation, and can reduce the extent of neuronal damage (Alessandrini et al. 1999). Primary neuronal culture literature also suggests that the MAP kinase pathway is relevant to excitotoxic damage *in vitro* (Bading and Greenberg 1991; Fiore et al. 1993; Kurino et al. 1995; Murray et al. 1998; Rosen et al. 1994; Xia et al. 1996). These reports indicate that glutamate signaling through its various ionotropic and/or metabotropic receptors results in p42/44 MAP kinase activation. Increased p44/42 MAP kinase activation induces immediate early

gene transcription (Xia et al. 1996) and is implicated in seizure activity-induced cell death of cultured hippocampal neurons (Murray et al. 1998).

The signaling pathways that link the NMDA receptor to p42/44 MAP kinase activation, or the downstream pathways which link p42/44 MAP kinase to delayed neurotoxicity, are not well understood. The upstream activators of p42/44 MAP kinases are MEK1 and MEK2 (Anderson et al. 1990; Crews, Alessandrini, and Erikson 1992; Zheng and Guan 1993). MEK1/2 are phosphorylated by the Raf family of kinases (Jaiswal et al. 1994; Moodie et al. 1993), which are activated by the Ras family of small GTP-binding proteins (Papin et al. 1995).

One candidate intermediate molecule that may couple NMDA receptor activation to the Ras/Raf/MEK/p42/44 MAPK signaling cascade is the calcium-dependent tyrosine kinase PYK2 (Lev et al. 1995). Increased intracellular calcium levels can activate PYK2, which can in turn activate MAP kinase signaling.

A second candidate intermediate that may link ion channel activation to MAP kinase signaling is calmodulin kinase (CaM-K). Two types of CaM-Ks are highly expressed in neurons, CaM-KII and CaM-KIV (Sakagami and Kondo 1993; Sola, Tusell, and Serratosa 1999). These protein kinases are activated upon binding of calcium and calmodulin, and they can regulate p38, JNK, and p42/44 MAP kinase activity (Enslen et al. 1996).

A third candidate intermediate molecule may be nitric oxide (NO). In cortical neurons, NMDA receptor coupling to NO production through PSD-95 is required for NMDA receptor-triggered neurotoxicity (Sattler et al. 1999). Increased NO production can also increase p42/44 MAP kinase activity (Lander et al. 1996).

Molecules that are downstream of p42/44 MAP kinase include transcription factors such as CREB, Elk-1, c-Jun, and c-Fos (Vanhoutte et al. 1999). The p42/44 MAP kinase pathway can also induce phosphorylation of cytoskeletal components such as neurofilaments (Li et al. 1999a), regulate synapsin I-actin interactions (Jovanovic et al. 1996), phosphorylate myelin basic protein (Ahn et al. 1991), and regulate the secretion of amyloid precursor protein (Desdouits-Magnen et al. 1998). Therefore, there are many potential mediators of neurotoxicity downstream of p42/44 MAP kinase activation.

A detailed understanding of the signaling pathways that are activated downstream of glutamate receptor stimulation would be useful for determining

efficient means of preventing hypoxia/ischemia-induced neuronal damage. Numerous attempts to study these pathways have been made toward this end. Lipton, U.S. Patent 5,506,231, describes a method of reducing damage to CNS neurons in a patient infected with human immunodeficiency virus by administration of a compound that antagonizes the NMDA receptor. This patent does not suggest neuroprotective effects by administration of a compound that modulates signal transduction pathway components downstream of the NMDA receptor. Maiese, U.S. Patent 5,519,035, describes Protein Kinase C inhibitors as neuroprotective from cerebral ischemia induced by nitric oxide administration. A model utilizing hippocampal neuronal cultures is described. Mahanthappa, WO 99/00117, describes compounds, including H89, that mimic the Hedgehog effects on the Patched-mediated signals, particularly inhibitors of protein kinase A (PKA) as neuroprotective agents. Liu, WO 99/58982, describes methods for identifying neuroprotective compounds that antagonize c-Jun N-termina Kinase (JNK) or mixed-lineage kinase (MLK) in neuronal cells, particularly HN33 hippocampal neuronal cells. Finally, Alessandrini, WO 99/34792, describes a mouse model of stroke in which focal cerebral ischemia is induced, and MEK1 inhibitors are administered to monitor neuroprotective effects.

Despite what is known about glutamate receptor-mediated excitotoxicity, much remains to be learned about its mechanisms of action and compounds that can selectively inhibit the neuronal cell death it causes.

Summary of the Invention

This invention provides a pharmaceutical composition comprising a pharmaceutically acceptable carrier and a compound having the formula

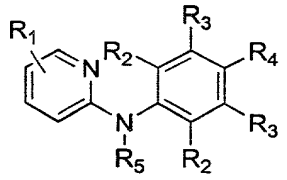

or a pharmaceutically acceptable salt thereof, wherein

(a) R_1 is H or a substituent bound at either the 5 or 6 ring position and selected from the group consisting of alkyl, alkenyl, alkynyl, thienyl, furanyl, pyrrolyl, phenyl, pyrimidinyl, substituted pyrimidinyl, pyridinyl, substituted

pyridinyl, phenyl alkenyl, substituted phenyl alkenyl, benzo[b]thien-2-yl, 2-benzofuranyl and substituted phenyl,

said substituted phenyl having the formula

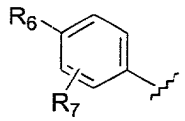

wherein (i) R_6 is selected from the group consisting of H, OH, halogen, alkylamino, dialkylamino, hydroxy-substituted dialkyl amino, lower alkyl, acidic lower alkyl, alkoxy, halogen-substituted lower alkoxy, phenyl and morpholinyl, and (ii) R_7 represents between one and four substituents which may be the same or different and are selected from the group consisting of H, halogen, amino, alkyl, lower alkyl, halogen-substituted lower alkyl, alkylamino, dialkylamino, acidic lower alkoxy, alkoxy, halogen-substituted lower alkoxy, alkoxy and phenylalkoxy, with the proviso that R_6 and R_7 may be fused to form 2-naphthyl or 1,3, benzodioxolyl;

(b) Each R_2 is independently H or lower alkyl;

(c) Each R_3 is independently selected from the group consisting of H, lower alkyl, amino, alkylamino, dialkylamino and lower alkoxy;

(d) R_4 is H, alkoxy or morpholinyl, with the proviso that R_4 may be fused with R_3 to form 2,3-dihydro-1,4-benzodioxinyl or 9-alkyl 9H carbazolyl; and

(e) R_5 is H or lower alkyl.

This invention also provides a method for reducing ischemic death in a cell population comprising contacting the cell with a prophylactically effective amount of the compound contained in the instant pharmaceutical composition.

This invention further provides a method for reducing neuronal cell death in response to a traumatic event comprising contacting the neuronal cell with a prophylactically effective amount of the compound contained in the instant pharmaceutical composition prior to, during, or within a suitable time period following the traumatic event.

This invention still further provides a method of reducing neuronal cell death in response to a traumatic event in a subject, comprising administering to the subject a prophylactically effective amount of the instant pharmaceutical composition prior to, during, or within a suitable time period following the traumatic event.

Finally, this invention provides an apparatus for administering to a subject the instant pharmaceutical composition comprising a container and the pharmaceutical composition therein, wherein the container has a device for delivering to the subject a prophylactic dose of the pharmaceutical composition.

Brief Description of the Figures

Figure 1. A: NMDA receptor-mediated functional intracellular calcium response. Filled square symbols represent the control, filled triangle symbols represent 100μM MK-80-1; B: [^{3}H]-MK-801 binding in differentiated P19 neurons.

Figure 2. A: P19 neuron viability experiment using Alamar Blue fluorescence measurements. B: Glutamate dose-response of death with alamar blue readings. Data presented as % control. C: MK-801 dose-dependent block.

Figure 3. A: Compound A, a p38 inhibitor, pretreatment dose response. B: U0126, a MEK1/2 inhibitor, pretreatment dose response.

Figure 4. A: U0126 does not block glutamate-induced calcium responses. B: U0126 does not block [3H]-MK-801 binding in P19 neurons.

Figure 5. A: U0126 post treatment time course of efficacy. B: Compound A post treatment time course of efficacy.

Figure 6. A: U0126 does not inhibit staurosporine-induced toxicity. Filled square symbols represent no compound; filled triangle symbols represent 10μM U0126. B: U0126 does not block A23187-induced toxicity. C: U0126 does not affect basal P19 neuron viability.

Figure 7. 2-pyridinamine and 4-pyrimidinamine compounds (listed by compound number) exhibit post-treatment delayed neuroprotection. Efficacy that is achieved at 2 hours post-glutamate treatment is equivalent to what is achieved when P19 neurons are pretreated with these compounds. This temporal profile matches that of the MEK inhibitor, U0126. Open, dotted bars represent pre treatment % NP; filled bars represent %NP 2 hours post treatment.

Detailed Description of the Invention

This invention provides a pharmaceutical composition comprising a pharmaceutically acceptable carrier and a compound having the formula

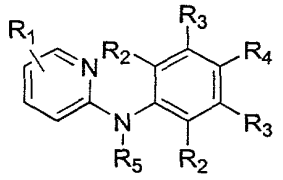

or a pharmaceutically acceptable salt thereof, wherein

(a) R_1 is H or a substituent bound at either the 5 or 6 ring position and selected from the group consisting of alkyl, alkenyl, alkynyl, thienyl, furanyl, pyrrolyl, phenyl, pyrimidinyl, substituted pyrimidinyl, pyridinyl, substituted pyridinyl, phenyl alkenyl, substituted phenyl alkenyl, benzo[b]thien-2-yl, 2-benzofuranyl and substituted phenyl,

said substituted phenyl having the formula

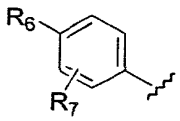

wherein (i) R_6 is selected from the group consisting of H, OH, halogen, alkylamino, dialkylamino, hydroxy-substituted dialkyl amino, lower alkyl, acidic lower alkyl, alkoxy, halogen-substituted lower alkoxy, phenyl and morpholinyl, and (ii) R_7 represents between one and four substituents which may be the same or different and are selected from the group consisting of H, halogen, amino, alkyl, lower alkyl, halogen-substituted lower alkyl, alkylamino, dialkylamino, acidic lower alkoxy, alkoxy, halogen-substituted lower alkoxy,

alkoxy and phenylalkoxy, with the proviso that R_6 and R_7 may be fused to form 2-naphthyl or 1,3, benzodioxolyl;

(b) Each R_2 is independently H or lower alkyl;

(c) Each R_3 is independently selected from the group consisting of H, lower alkyl, amino, alkylamino, dialkylamino and lower alkoxy;

(d) R_4 is H, alkoxy or morpholinyl, with the proviso that R_4 may be fused with R_3 to form 2,3-dihydro-1,4-benzodioxinyl or 9-alkyl 9H carbazolyl; and

(e) R_5 is H or lower alkyl.

In one embodiment of the instant pharmaceutical composition, R_1 is a substituted phenyl at the 5 ring position, and each R_2 is H. In another embodiment, R_4 is morpholinyl. In a further embodiment, each R_3 is a lower alkoxy and R_4 is a lower alkoxy. In still a further embodiment, R_1 is at the 6 ring position, each R_2 is H, and preferably, each R_3 and R_4 are lower alkoxy.

In the preferred embodiment of the instant pharmaceutical composition, the compound contained therein is selected from the following group, whose structures are set forth in the Experimental Details:

5-(3-ethoxyphenyl)-N-(3,4,5-trimethoxyphenyl)-2-pyridinamine;
N-[4-(4-morpholinyl)phenyl]-5-(2-naphthyl)-2-pyridinamine;
5-benzo[b]thien-2-yl-N-[4-(4-morpholinyl)phenyl]-2-pyridinamine;
5-[3,5-bis(trifluoromethyl)phenyl]-N-[4-(4-morpholinyl)phenyl]-2-pyridinamine;
5-[4-(4-morpholinyl)phenyl]-N-[4-(pentyloxy)phenyl]-2-pyridinamine;
5-[4-(dimethylamino)phenyl]-N-[4-(pentyloxy)phenyl]-2-pyridinamine;
5-[4-(dimethylamino)phenyl]-N-(4-methoxyphenyl)-2-pyridinamine;
5-(1,3-benzodioxol-5-yl)-N-[4-(pentyloxy)phenyl]-2-pyridinamine;
4-[6-[[4-(pentyloxy)phenyl]amino]-3-pyridinyl]-benzenepropanoic acid;
5-(2-methoxyphenyl)-N-[4-(pentyloxy)phenyl]-2-pyridinamine;
N-(2,3-dihydro-1,4-benzodioxin-6-yl)-5-[(E)-2-phenylethenyl]-2-pyridinamine;
N-[6-[3-(dimethylamino)phenyl]-2-pyridinyl]-9-ethyl-9H-carbazol-3-amine;
6-(3-ethoxyphenyl)-N-(3,4,5-trimethoxyphenyl)-2-pyridinamine;

6-[3-(trifluoromethoxy)phenyl]-N-(3,4,5-trimethoxyphenyl)-2-pyridinamine;
6-(1,3-benzodioxol-5-yl)-N-(3,4,5-trimethoxyphenyl)-2-pyridinamine;
6-phenyl-N-(3,4,5-trimethoxyphenyl)-2-pyridinamine;
6-(3,4-dimethoxyphenyl)-N-(3,4,5-trimethoxyphenyl)-2-pyridinamine;
6-(3,4-dimethylphenyl)-N-(3,4,5-trimethoxyphenyl)-2-pyridinamine;
N-(4,5-dimethoxy-2-methylphenyl)-6-(3,4-dimethylphenyl)-2-pyridinamine;
6-(2-naphthyl)-N-(3,4,5-trimethoxyphenyl)-2-pyridinamine;
6-(2-phenoxyphenyl)-N-(3,4,5-trimethoxyphenyl)-2-pyridinamine; and
6-[(E)-2-phenylethenyl]-N-(3,4,5-trimethoxyphenyl)-2-pyridinamine.

Unless specified otherwise, as used herein, the term "alkyl" refers to a saturated straight, branched or cyclic substituent consisting solely of carbon and H. Lower alkyl refers to an alkyl containing 1 to 4 carbon atoms. The term "alkenyl" refers to an unsaturated straight, branched or cyclic substituent consisting solely of carbon and H that contains at least one double bond. The term "alkynyl" refers to an unsaturated straight, branched or cyclic substituent consisting solely of carbon and H that contains at least one triple bond.

The term "alkoxy" refers to O-alkyl where alkyl is as defined. The term "alkylthio" refers to S-alkyl where alkyl is as defined. An acidic alkyl is a carbon chain with a terminal COOH group.

As used herein, the term "alkylamino" shall mean an alkyl substituted amine group. Similarly, the term "dialkylamino" shall mean an amino group substituted with two independently selected alkyl groups. The term "hydroxy substituted dialkylamino" shall refer to a dialkylamino group wherein either or both of the alkyl groups are independently substituted with a hydroxy group, independently at any of the carbon atoms of the alkyl group(s).

The term "halo" means fluoro, chloro, bromo and iodo. The symbol "Ph" or "PH" refers to phenyl.

When a particular group is "substituted" (e.g., aryl, heterocycloalkyl, heteroaryl, and the like), that group may have one or more substituents, preferably from one to five substituents, more preferably from one to three substituents, most preferably from one to two substituents, independently selected from the list of substituents.

With reference to substituents, the term "independently" means that when more than one of such substituents is possible, such substituents may be the same or different from each other.

For the purposes of this invention, the pyridine ring system shall have the following numbering.

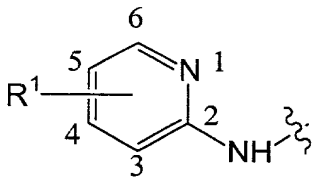

The compounds contained in the instant pharmaceutical compositions are exemplified in the Experimental Details section below. These compounds are commercially available from BioFocus PCC (UK) as part of a chemical library. Alternatively, the compounds exemplified below can be prepared using known methods.

As used herein, the phrase "pharmaceutically acceptable salt" means a salt of the free base which possesses the desired pharmacological activity of the free base and which is neither biologically nor otherwise undesirable. These salts may be derived from inorganic or organic acids. Examples of inorganic acids are hydrochloric acid, nitric acid, hydrobromic acid, sulfuric acid, and phosphoric acid. Examples of organic acids are acetic acid, propionic acid, glycolic acid, lactic acid, pyruvic acid, malonic acid, succinic acid, malic acid, maleic acid, fumaric acid, tartaric acid, citric acid, benzoic acid, cinnamic acid, mandelic acid, methanesulfonic acid, ethanesulfonic acid, p-toluenesulfonic acid, methyl sulfonic acid, salicyclic acid and the like.

The instant pharmaceutical composition can be prepared according to conventional pharmaceutical techniques. The pharmaceutically acceptable carrier therein may take a wide variety of forms depending on the form of preparation desired for administration, such as systemic administration, including but not limited to intravenous, oral, nasal or parenteral. In preparing the compositions in oral dosage form, any of the usual pharmaceutical carriers may be employed, such as water, glycols, oils, alcohols, flavoring agents, preservatives, coloring agents, syrup and the like in the case of oral liquid preparations (for example, suspensions, elixirs and solutions), or

carriers such as starches, sugars, diluents, granulating agents, lubricants, binders, disintegrating agents and the like in the case of oral solid preparations (for example, powders, capsules and tablets).

Because of their ease of administration, tablets and capsules represent an advantageous oral dosage unit form, wherein solid pharmaceutical carriers are employed. If desired, tablets may be sugar-coated or enteric-coated by standard techniques. For parenterals, the carrier will usually comprise sterile water, though other ingredients for solubility or preservative purposes may also be included. Injectable suspensions may also be prepared, wherein appropriate liquid carriers, suspending agents and the like may be employed. The compounds may also be administered in the form of an aerosol.

This invention also provides a method of reducing the likelihood of a cell's undergoing ischemic death comprising contacting the cell with a prophylactically effective amount of the compound contained in the instant pharmaceutical composition.

As used herein, the term "ischemic death", when referring to a cell, means death caused by a lack of oxygen. Ischemic cell death can result, for example, from hypoxic conditions. *In vivo* or *ex vivo* ischemia of cells or entire tissues can result from, among other things, localized anemia due to interference of the blood supply caused by blood vessel obstruction, destruction or constriction. Ischemic death and its morphologic characteristics are well known and identifiable to those with ordinary skill in the art.

As used herein, a "prophylactically effective amount" of the instant pharmaceutical composition, or compound therein, means an amount that reduces the incidence of cell death in a population of cells. The instant pharmaceutical composition will generally contain a per dosage unit (e.g., tablet, capsule, powder, injection, teaspoonful and the like) from about 0.001 to about 100 mg/kg. In one embodiment, the instant pharmaceutical composition contains a per dosage unit of from about 0.01 to about 50 mg/kg of compound, and preferably from about 0.05 to about 20 mg/kg. Methods are known in the art for determining prophylactically effective doses for the instant pharmaceutical composition. The effective dose for administering the

pharmaceutical composition to a human, for example, can be determined mathematically from the results of animal studies.

A "cell population" as used herein refers to cells in vitro such as in a culture vessel or in vivo as part of a body fluid or as an intact tissue or organ. The cell population can be homogenous (comprising of one cell type) or heterogenous (comprising a mixed cell type population). Preferred cell populations are heterogenous cell populations that comprise at least one cell type that has been identified as being protected from ischaemic death in the presence of the compounds of this invention.

In one embodiment of the instant method, the cells making up the cell populations are preferably mammalian cells and more preferably human cells. The cells that make up a cell population that demonstrates reduced ischaemic injurly in response to a traumatic invent include, but are not limited to, cell populations comprising at least one cell selected from the group consisting of a neuronal cell, a glial cell, a cardiac cell, a lymphocyte, a macrophage and a fibroblast. In the preferred embodiment, the cell is a neuronal cell.

This invention also provides a method of reducing neuronal cell death in response to a traumatic event comprising contacting the neuronal cell with a prophylactically effective amount of the compound contained in the instant pharmaceutical composition prior to, during, or within a suitable time period following the traumatic event.

Both these instant methods can be performed *in vitro*, *ex vivo*, or *in vivo*. As used herein, contacting a cell with an agent "*in vitro*" includes, by way of example, contacting such agent with a cell that is in a single cell culture, a mixed cell culture or a primary cell tissue culture. Contacting a cell with an agent "*ex vivo*" includes, by way of example, contacting such agent with a cell that is part of an organized tissue or organ maintained outside the body of the subject from which it originates. Contacting a cell with an agent "*in vivo*" means contacting such agent with a cell present within a subject.

This invention further provides a method for reducing neuronal cell death in response to a traumatic event in a subject, comprising administering to the subject a prophylactically effective amount of the instant pharmaceutical composition prior to, during, or within a suitable time period following the traumatic event. The term "subject" includes, without limitation, any animal or artificially modified animal. In the preferred embodiment, the subject is a human.

The route of administering the instant pharmaceutical composition to a subject is preferably systemic, including, for example, intravenous (iv), subcutaneous (sc) and oral administration. In one embodiment, the instant composition is administrated directly to the nervous system. This administration route includes, but is not limited to, the intracerebral, intraventricular, intracerebroventricular, intrathecal, intracisternal, intraspinal and/or peri-spinal routes of administration, which can employ intracranial and intravertebral needles, and catheters with or without pump devices. Infusion doses can range, for example, from about 1.0 to 1.0 x 10^4 μg/kg/min of instant compound, over a period ranging from several minutes to several days. For topical administration, the instant compound can be mixed with a pharmaceutical carrier at a concentration of, for example, about 0.1 to about 10% of drug to vehicle.

In the instant method, the neuronal cell death-causing traumatic event includes, for example, a medical disorder, a physical trauma, a chemical trauma and a biological trauma.

Examples of neuronal cell death-causing medical disorders include perinatal hypoxic-ischemic injury, cardiac arrest, stroke/ischemic attack, hypoglycemia-induced neuropathy, cardiac surgery-induced cerebral ischemia, post traumatic stress disorder, stress-induced memory impairment, chronic epilepsy, multiple sclerosis, Parkinson's disease, diabetic peripheral neuropathy, neuropathic pain, Bells' palsy, sick sinus syndrome, Alzheimer's disease, Pick's disease, diffuse Lewy body disease, Cruzfeld's Jacobs and other diseases of protein aggregation, progressive supranuclear palsy (Steel-Richardson syndrome), multisystem degeneration (Shy-Drager syndrome), amyotrophic lateral sclerosis (ALS), degenerative ataxias, cortical basal degeneration, ALS–Parkinson's–Dementia complex of Guam, subacute sclerosing panencephalitis,

Huntington's disease, synucleinopathies (including multiple system atrophy), primary progressive aphasia, striatonigral degeneration, Machado-Joseph disease, spinocerebellar ataxia type 3, olivopontocerebellar degenerations, Gilles De La Tourette's disease, bulbar and pseudobulbar palsy, spinal and spinobulbar muscular atrophy (Kennedy's disease), primary lateral sclerosis, familial spastic paraplegia, Werdnig-Hoffmann disease, Kugelberg-Welander disease, Tay-Sach's disease, Sandhoff disease, familial spastic disease, neuroleptic malignant syndrome, Wohlfart-Kugelberg-Welander disease, spastic paraparesis, progressive multifocal leukoencephalopathy, AIDS-related dementia, sick sinus syndrome, post herpetic neuropathy, viral meningitis, bacterial meningitis, prion diseases, and familial dysautonomia (Riley-Day syndrome).

Neuronal cell death-causing physical traumas include, for example, focal brain trauma, diffuse brain trauma, spinal cord injury, cerebral infarction, embolic occlusion, thrombotic occlusion, reperfusion, intracranial hemorrhage, whiplash, shaken infant syndrome, and radiation-induced peripheral nerve damage.

Neuronal cell death-causing chemical traumas include, for example, exposure to alcohol, chemotherapeutic agents, war gas, lead, cyanoacrylate, polyacrylamide, and toxic inhalants. Finally, neuronal cell death-causing biological traumas include, for example, exposure to HIV, herpes virus, and meningitis-causing bacteria and viruses.

In practicing the instant method, the pharmaceutical composition can be administered to the subject prior to, during or subsequent to the traumatic event. As used herein the term "subsequent" refers to any point in time beginning with the traumatic event and continuing until the potential of cell death resulting from the traumatic event has diminished.

Finally, this invention provides an apparatus for administering to a subject any of the instant pharmaceutical composition comprising a container and the pharmaceutical composition therein, wherein the container has a device for delivering to the subject a prophylactic dose of the pharmaceutical composition. In the preferred embodiment, the device for delivering the pharmaceutical composition is a syringe.

Ideally, the instant apparatus is a single-use, predosed auto-injectable device containing the instant composition. Such a device would be useful, for example, in a mobile ambulatory unit or for administration to a person at risk for a neurotoxic event. Mechanical auto-injectable devices are well known in the art and are exemplified, for example, by an EpiPen® device (Meridian Medical Technologies Inc.), which is an auto-injectable device containing epinephrin for individuals subject to anaphalactic shock.

This invention will be better understood by reference to the Experimental Details that follow, but those skilled in the art will readily appreciate that these are only illustrative of the invention as described more fully in the claims which follow thereafter. Additionally, throughout this application, various publications are cited. The disclosure of these publications is hereby incorporated by reference into this application to describe more fully the state of the art to which this invention pertains.

Experimental Details

Example 1

Commercially Available 2-Pyridinamines

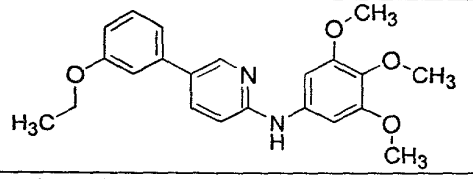	2-pyridinamine, 5-(3-ethoxyphenyl)-*N*-(3,4,5-trimethoxyphenyl)- (Cmpd 12)
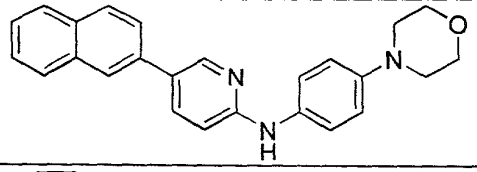	2-pyridinamine, *N*-[4-(4-morpholinyl)phenyl]-5-(2-naphthyl)- (Cmpd 25)
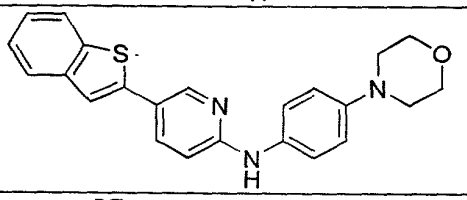	2-pyridinamine, 5-benzo[*b*]thien-2-yl-*N*-[4-(4-morpholinyl)phenyl]- (Cmpd 22)
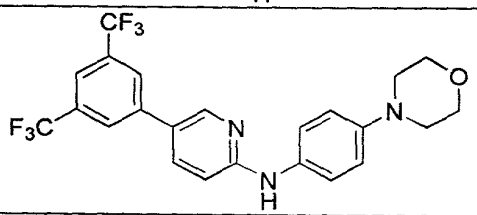	2-pyridinamine, 5-[3,5-bis(trifluoromethyl)phenyl]-*N*-[4-(4-morpholinyl)phenyl]- (Cmpd 21)

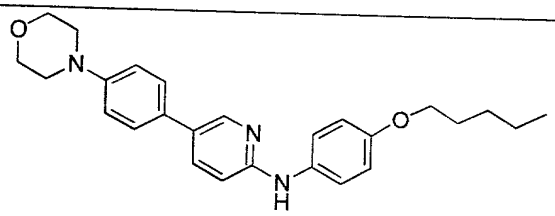	2-pyridinamine, 5-[4-(4-morpholinyl)phenyl]-*N*-[4-(pentyloxy)phenyl]- (Cmpd 6)
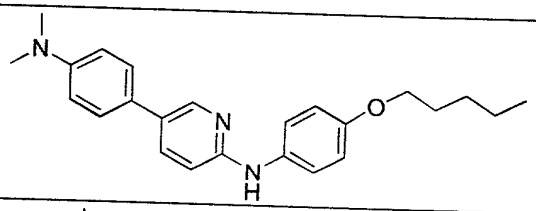	2-pyridinamine, 5-[4-(dimethylamino)phenyl]-*N*-[4-(pentyloxy)phenyl]- (Cmpd 7)
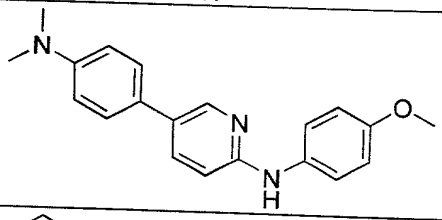	2-pyridinamine, 5-[4-(dimethylamino)phenyl]-*N*-(4-methoxyphenyl)- (Cmpd 8)
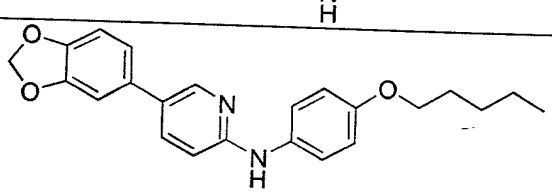	2-pyridinamine, 5-(1,3-benzodioxol-5-yl)-*N*-[4-(pentyloxy)phenyl]- (Cmpd 13)
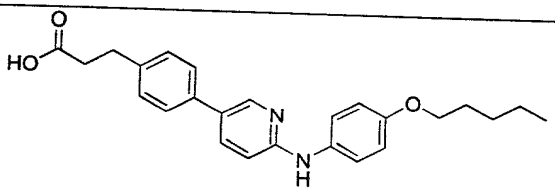	benzenepropanoic acid, 4-[6-[[4-(pentyloxy)phenyl]amino]-3-pyridinyl]- (Cmpd 10)
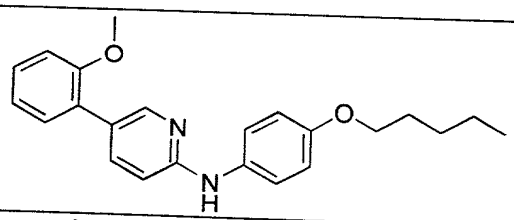	2-pyridinamine, 5-(2-methoxyphenyl)-*N*-[4-(pentyloxy)phenyl]- (Cmpd 14)
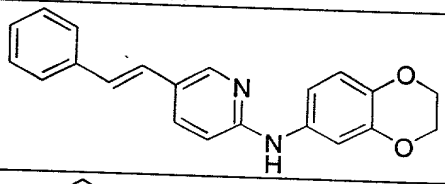	2-pyridinamine, *N*-(2,3-dihydro-1,4-benzodioxin-6-yl)-5-[(*E*)-2-phenylethenyl]- (Cmpd 88)
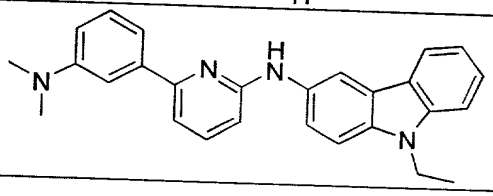	9*H*-carbazol-3-amine, *N*-[6-[3-(dimethylamino)phenyl]-2-pyridinyl]-9-ethyl- (Cmpd 104)

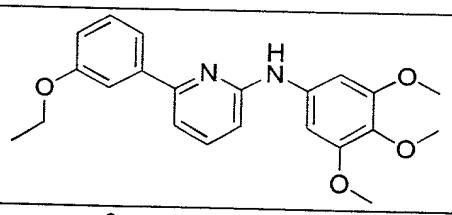	2-pyridinamine, 6-(3-ethoxyphenyl)-*N*-(3,4,5-trimethoxyphenyl)- (Cmpd 114)
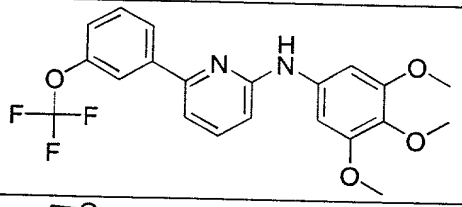	2-pyridinamine, 6-[3-(trifluoromethoxy)phenyl]-*N*-(3,4,5-trimethoxyphenyl)- (Cmpd 118)
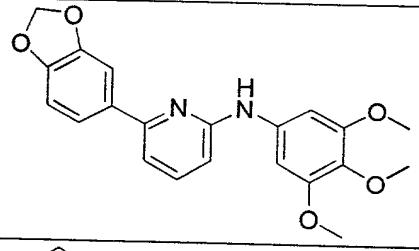	2-pyridinamine, 6-(1,3-benzodioxol-5-yl)-*N*-(3,4,5-trimethoxyphenyl)- (Cmpd 120)
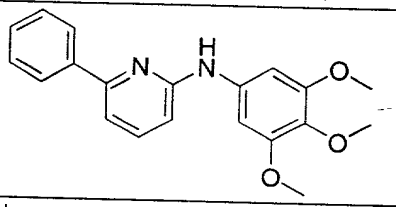	2-pyridinamine, 6-phenyl-*N*-(3,4,5-trimethoxyphenyl)- (Cmpd 122)
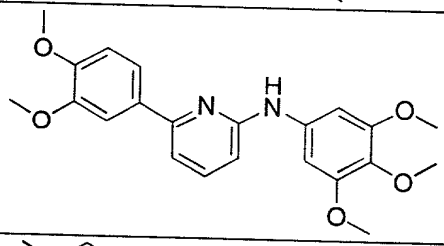	2-pyridinamine, 6-(3,4-dimethoxyphenyl)-*N*-(3,4,5-trimethoxyphenyl)- (Cmpd 124)
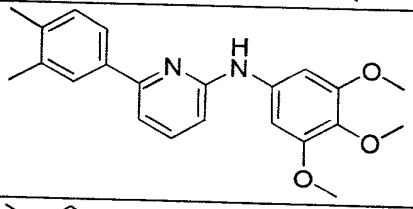	2-pyridinamine, 6-(3,4-dimethylphenyl)-*N*-(3,4,5-trimethoxyphenyl)- (Cmpd 126)
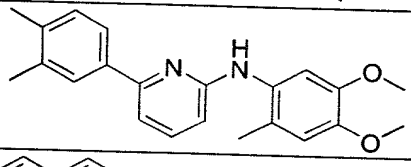	2-pyridinamine, *N*-(4,5-dimethoxy-2-methylphenyl)-6-(3,4-dimethylphenyl)- (Cmpd 127)
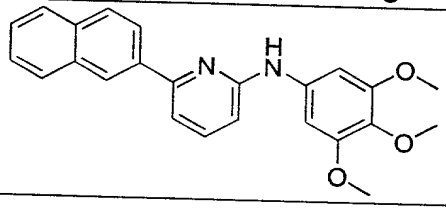	2-pyridinamine, 6-(2-naphthyl)-*N*-(3,4,5-trimethoxyphenyl)- (Cmpd135)

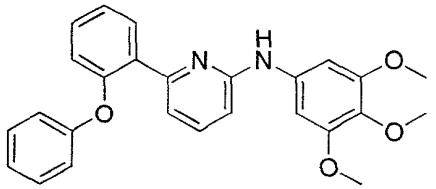	2-pyridinamine, 6-(2-phenoxyphenyl)-*N*-(3,4,5-trimethoxyphenyl)- (Cmpd 138)
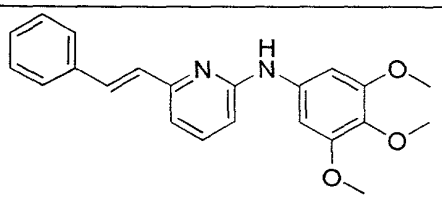	2-pyridinamine, 6-[(*E*)-2-phenylethenyl]-*N*-(3,4,5-trimethoxyphenyl)- (Cmpd144)

Example 2
Characterization of Differentiated P19 Cells

P19 Cell Differentiation

P19 cells are a pluripotent embryonal carcinoma line that can be induced to differentiate relatively rapidly into post-mitotic neurons in the presence of high dose retinoic acid (Jones-Velleneuve et al. 1982; Jones-Villeneuve et al. 1983; McBurney and Rogers 1982). They are the murine equivalent of human NT-2N neurons, which are also derived from retinoic acid differentiation of teratocarcinoma precursor cells. Differentiated NT-2N neurons, perhaps the better known of the two teratocarcinoma-derived neuronal lines, express a wide variety of neuronal markers, and undergo NMDA receptor-mediated, hypoxia-induced excitotoxic cell death (Pleasure and Lee 1993; Pleasure, Page, and Lee 1992; Rootwelt et al. 1998). Like NT-2Ns, differentiated P19 neurons also express a wide variety of neuronal markers, exhibit NMDA receptor-mediated intracellular calcium responses to agonists, and undergo excitotoxicity (Canzoniero et al. 1996; Grobin et al. 1999; Morley et al. 1995; Ray and Gottlieb 1993; Turetsky et al. 1993).

P19 cells were bought from ATCC (Manassas, VA). They were grown on 150 cm^2 tissue culture flasks in Dulbecco's Modified Eagle Medium (DMEM, Gibco BRL) supplemented with 10% fetal bovine serum, glutamine (2 mM), sodium pyruvate (1 mM), sodium bicarbonate (0.15% w/v), and penicillin/streptomycin (50 units/mL) in an atmosphere of 5% CO_2 at 37°C.

On day 1 of the differentiation protocol, confluent P19 cells were split to 50-70% confluency in growth medium. On day 2 of the protocol, 10 μM all-trans-retinoic acid (ATRA, Sigma) and 10 μM MK-801 were added to the growth medium. 10 μM MK-801 was included at this stage to prevent cell death in differentiating neurons that

begin to express NMDA receptors. On day 4, fresh growth medium was placed on the cells, with fresh ATRA and MK-801. On day 5, cells were dissociated from the tissue culture flask by washing 4 times with calcium and magnesium-free phosphate-buffered saline, and adding 4 mL of non-enzymatic cell dissociation solution (Sigma).

Once dissociated, cells were placed in 40 mLs of differentiation medium. Differentiation medium consisted of Neurobasal medium (Gibco BRL) supplemented with 1% N-2 supplement (Gibco BRL), 0.1 % trace elements B (Mediatech), 1 mM cadmium sulfate (Sigma), 2 mM glutamine, sodium pyruvate (1 mM), sodium bicarbonate (0.15% w/v), and 1% antibiotic/antimycotic (Gibco BRL). 10 μM cytosine-D-arabinofuranoside was added to the differentiation medium to prevent growth of undifferentiated cells. No MK-801 was present from this point onward. Cells were triturated 20 times, then were split 1:4 into 96 well plates, or split 1:3 into 100 mm tissue culture dishes. Four days after replating, the cells were optimal for compound addition, and were assayed 24 hours later.

RT-PCR

Total RNA was isolated from 100 mm tissue culture dishes of differentiated P19 neurons or undifferentiated P19 cells using the QIAGEN RNeasy Mini kit according to manufacturer's protocols. RT-PCR amplification of murine NMDA receptor subunits was obtained from 250 ng total RNA template isolated from undifferentiated P19 cells, cells at 4 days after retinoic acid (ATRA) induction, and cells at 9 days after ATRA induction. One-step RT-PCR reactions were set up using the LightCycler™-RNA Amplification kit SYBR Green I kit (Boehringer Mannheim), according to manufacturer's protocols. Real time RT-PCR reactions were carried out in LightCycler™ glass capillaries using the LightCycler™ instrument and 250 ng template RNA (Boehringer Mannheim). The reverse transcriptase reaction was carried out for 10 min at 55°C. PCR was carried out for 30 cycles: annealing temperature was 50°C, extension temperature was 72°C, and melting temperature was 80°C. Reactions were compared to an H_2O-negative control for each primer set. 5 μL of reaction product were removed, and run on 1x TBE agarose gels. The primer sets for the various mouse NMDA receptor subunits used include zeta 1 and epsilons 1-4.

RNA samples from 4-day and 9-day post retinoic acid treatmnet, undifferentiated smaples and control sampes were separated by electrophoresis and probed with zeta1, epslon 1 and epsilon 2 internal primers

RT-PCR of NMDA receptor subunits from total RNA samples revealed that retinoic acid induction of differentiation also induces mRNA expression of zeta1, epsilon1, and epsilon2 mRNAs. Data was summarized using 3 separate experiments.

Western Blots

Media was aspirated from cells plated onto 100 mm tissue culture dishes. Cells were harvested in RIPA lysis buffer (100mM Tris HCL pH 7.5, 150 mM NaCl, 1 mM EDTA, 1% Triton X-100, 10% sodium deoxycholate, 0.1% sodium dodecyl sulfate). Each sample was sonicated for 20 seconds, Laemmli sample buffer (BioRad) was added to a final 1x concentration, and samples were incubated for 10 minutes at 95^{0}C. Samples to be probed with NMDA receptor antibodies (polyclonals against rat NR1, NR2A, and NR2B obtained from Chemicon) were electrophoresed on 6% tris-glycine pre-cast gels (NOVEX). Samples to be probed with p42/44 MAP kinase antibodies (New England BioLabs) were electrophoresed on 12% tris-glycine pre-cast gels (NOVEX). Electrophoresis was carried out in a NOVEX apparatus for 1.5 hours at 200 volts. Proteins were transferred to polyvinylidene difluoride membrane (PVDF, NOVEX) using a BioRad wet transfer device for 1 hour at 100 volts. Prior to transfer, PVDF membranes were dipped in 100% methanol for 1 minute, then soaked in transfer buffer for 5 minutes. After transfer, membranes were removed and were slowly shaken in blocking solution (5% milk, 0.05% tween-20 in phosphate buffered saline) at 4^{0}C overnight. Membranes were then washed once with PBS-tween, and primary antibodies 1:1000 in PBS-tween with 5 % milk were incubated for 1 hour at room temperature. Membranes were washed 4x for 15 minutes at room temperature. Secondary antibodies coupled to horseradish peroxidase were incubated for about 45 minutes at room temperature in PBS-tween with 5 % milk. Membranes were then washed 4x for 15 minutes at room temperature. Blots were developed using ECL plus (Amersham), and exposed to film.

Western blot analysis was performed for NMDA receptor subunit protein in P19 cell lysates harvested following 4-days or 9-days of retinoic acid exposure. Appropriately sized bands (Zeta1 = ~ 120 kDa, Epsilon1 and Epsilon 2 = ~ 180 kDa)

were detectable from terminally differentiated P19 neuron lysates, but not from undifferentiated cell lysates. The data was representative of 3 separate experiments with similar results.

Western blot analysis revealed that terminally differentiated P19 neurons express detectable levels of zeta1, epsilon1, and epsilon 2 proteins. Epsilon3 and epsilon4 mRNAs or proteins were not detectable at any time in these cells.

These data demonstrate that such methods of differentiating P19 cells into neurons successfully result in the functional expression of NMDA receptors at the levels of mRNA, protein, MK-801 sensitive agonist-induced intracellular calcium responses, and MK-801 sensitive glutamate toxicity. These data are in very good agreement with the literature. Interestingly, however, in addition to zeta1 and epsilon2 expression, reliable expression of the epsilon1 subunit of the NMDA receptor was also achieved, which expression has not yet been achieved with other reported methods of P19 cell differentiation (Ray and Gottlieb 1993). The presence of all three subunits more closely resembles expression patterns observed in adult rodent forebrain regions, including cortex and hippocampus (Ishii et al. 1993; Laurie et al. 1995; Monyer et al. 1994; Monyer et al. 1992; Standaert et al. 1994).

Example 3
Differentiated P19 Excitotoxicity Assay

Cells were loaded with 5 μM Fura-2-AM (Molecular Probes) for 1 hr at 37°C. They were washed once with Hank's balanced salt solution (HBSS, Gibco BRL), and assayed in HBSS buffer. Cells were placed onto the stage of a modified ATTOFLUOR™ Imager (Atto Instruments, Rockville Pike, MD). High speed, dual excitation of fura-2 was carried out using a RATIOARC™ High-Speed Excitor (Atto Instruments). Mercury lamp light was passed through 334 nm or 380 nm bandpass filters (10 nm band width), and then passed through a 20x objective (Zeiss, Plan-Apochromat, NA=0.75) at a rate of 2.5 Hz. Emitted light was transmitted through a 400 nm dichroic mirror, and collected to an ATTOFLUOR™ intensified CCD camera. Ratio-images were acquired, and the average intensity of the images when excited at 334nm and 380nm was analyzed using ATTOFLUOR RATIOVISION™ software (Atto Instruments, Rockville, MD).

Changes of the Fura-2 330nm/380nm intensity ratio were plotted when 9 days post-ATRA P19 neurons were treated with 3 mM glutamate, 1 mM glycine in the presence or absence of 100 μM MK-801. MK-801 was administered 24 hours prior to assay. Traces are the average ± standard error from three separate experiments for each condition. Terminally differentiated P19 neurons expressed NMDA receptor subunits that form functional NMDA receptors, as illustrated by using fura-2 imaging to detect increases in intracellular calcium levels upon addition of NMDA receptor agonists (Figure 1A). The selective NMDA receptor channel blocker, MK-801, significantly inhibited this response (Figure 1A). In addition P19 neurons expressed specific binding sites for the NMDA receptor. MK-801 inhibition of [^{3}H]-MK-801 binding was assayed in P19 membranes. MK-801 concentrations are expressed as 10^{-x} Molar. Data points represent the mean ± standard error from eight experiments. % control = ((CPM – CPM_{bottom})/(CPM_{top}-CPM_{bottom})) X 100. (Figure 1B). MK-801 inhibition was concentration-dependent, and 100% inhibition was achieved.

Control P19 neuron cell bodies and processes stain brightly with the live cell cytoplasmic dye carboxyfluorescein diacetate (CFDA). P19 neurons at 9 days post ATRA induction were labeled with CFDA, and then imaged in confocal mode using an Attofluor Imager. Control cells were treated with vehicle for 24 hours, glutamate cells received 3 mM glutamate in the presence of 1 mM glycine for 24 hours, and glutamate + U0126 cells received 10 μM U0126 concurrent with 3 mM glutamate and 1 mM glycine for 24 hours. Images were taken from control alive, glutamate treated, dead and U0126-protected cells stained with fluorescein diacetate in 3 separate experiments. P19 neuron cell bodies characteristically clumped together into tight aggregates when plated onto plain tissue culture plastic. Networks of extensive processes connected clusters of neuronal cell bodies. P19 neurons treated with toxic concentrations of glutamate and glycine for 24 hours exhibited fluorescence staining in isolated cell bodies, processes were undetectable, and extensive cellular debris was evident. Relative levels of cell death were measured rapidly and quantitatively on a plate reader using the live cell fluorescent dye alamar blue (Figures 2B).

Alamar Blue fluorescence, an indicator of cell viability, was used to determine cell viability after an NMDA-induced cytotoxic insult. Counts from a single 96 well plate where 32 wells received vehicle control, 32 wells received 3 mM glutamate and 1 mM glycine for 24 hours, and 32 wells received 5 μM A23187 for 24 hours are shown

in Figure 2A. Glutamate and A23187 conditions were significantly different from control as determined by one-way ANOVA with Tukey post-hoc analysis carried out using GRAPHPAD™ software. These data indicate a typical 60% reduction in Alamar blue fluorescence when cells were treated with glutamate and glycine. However, since raw fluorescence counts vary from experiment to experiment, Figures 2A, 2B, and 2C are expressed as a percent of control.

Glutamate toxicity dose response in the presence of a constant 1 mM glycine concentration was measured in the differentiated P19 neurons. The curve generated through the data points is the average of 6 separate dose response curves. Data points are represented as the percent of control cells ± standard error. % control = $(([Glutamate]_{exp} - [Glutamate]_{max}) / (Control_{vehicle} - [Glutamate]_{max})) \times 100$. Glutamate toxicity EC50 was calculated to be 8.1 μM [lower 95% confidence interval = 3.5 μM; upper 95% confidence interval = 19 μM]. These data demonstrate that 24 hours of glutamate treatment killed P19 neurons dose-dependently in the presence of a constant dose of glycine (Figures 2A,2B). Glycine alone did not affect P19 neuron viability.

The NMDA receptor blocker, MK-801, dose-dependently protected against glutamate toxicity in P19 neurons (Figure 2D). MK-801 dose-dependent inhibition of 3 mM glutamate and 1 mM glycine-induced P19 neuron death. % Neuroprotection = $((\text{Inhibitor in the presence of Glutamate}_{max} - [Glutamate]_{max}) / (Control_{vehicle} - [Glutamate]_{max})) \times 100$. Data points are the average ± standard error of three separate experiments. Maximal MK-801 protection achieved was close to control levels.

These data demonstrate that glutamate toxicity in P19 neurons requires NMDA receptor activation, since the toxicity is completely blocked in the presence of the specific NMDA receptor antagonist MK-801. However, the data do not exclude the possibility that AMPA or kainate receptors may also be activated by glutamate and contribute to the excitotoxicity. This possibility would be consistent with data from primary neuronal culture, which reports that intracellular calcium responses to glutamate agonists involve multiple components (Courtney, Lambert, and Nicholls 1990). Such components include AMPA/kainate receptor activation, membrane depolarization, voltage-gated calcium channel activation, relief of NMDA receptor magnesium block, and NMDA receptor activation. However, even with such a high level of complexity, in many primary neuronal models, glutamate excitotoxicity signals

through the NMDA receptor and requires its activation to result in neuronal death (Tymianski et al. 1993), as is the case for P19 neuron model system.

These cells were used to measure the effects of various known kinase inhibitors (Compound Identification (ID) column in Table I) upon cytotoxicity-induced by NMDA. First, P19 cells were differentiated as described in Example 2. Then cells were exposed to 3 mM of glutamate in the presence of 1 mM glycine.

Cell viability was determined. Compounds that prevented excitotoxicity were determined by measuring the percentage of viable cells compared to differentiated P19 cells that were not presented with a toxic insult (Table I).

Cell viability was measured using two methods. The first method was a confocal, single-cell fluorescence imaging-based method using the live cell dye carboxy-fluorescein diacetate (CFDA). CFDA labels the cell bodies and processes of living cells. Therefore, live cells exhibit extensive CFDA labeling, whereas dead cells exhibit much less CFDA staining. CFDA fluorescence was measured using a modified Attofluor Imager device (Atto Instruments, Rockville Pike, MD). Cells were labeled with 1 uM CFDA for 15 min in media, then placed onto the stage of the Attofluor microscope. The dye was excited by light from a mercury lamp source passed through a 488 nm bandpass filter of 10 nm band width, passed through a CARV real-time confocal spinning disk module (Atto Instruments, Rockville, MD), and then passed through a 40x oil immersion objective (Zeiss Fluar, NA=1.3). Emitted light was transmitted through a 495 nm dichroic mirror, collected to an Attofluor intensified CCD camera, and images were visualized using Attofluor RatioVision software (Atto Instruments, Rockville, MD).

The second method for measuring cell viability was a plate reader method. Cells plated into black 96 well plates (Packard viewplates) are loaded with 5 % Alamar Blue dye (Biosource International). Alamar Blue is a dye that takes advantage of mitochondrial reductases to convert non-fluorescent resazurin to fluorescent resorufin (excitation 535 nm, emission 580 nm). Baseline fluorescence counts were read at room temperature in a Wallac plate reader immediately after addition of Alamar blue. Fluorescence counts of cell viability were taken the same way after 1 hour incubation at 37°C. Fluorescence was expressed as a percent of control, untreated cells after subtraction of background fluorescence. Live/dead cells were confirmed visually with a light microscope.

As used in Table I below, Compound A shall mean the compound have the formula

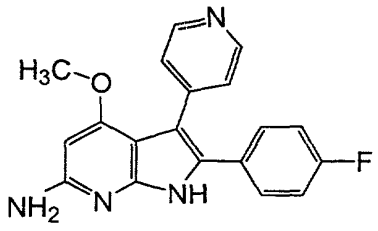

5

Table I
Comparison of Kinase Inhibitor Activity to Neuroprotective Activity

Compound ID	Enzyme target	Activity	Potency	IC50 for Neuropro-tection [lower-upper 95% C.I.]	Maximal Efficacy for Neuropro tection
Compound A	p38 kinase	Inhibitor	IC50~10 nM	9.7 μM [5.8-16.3]	>80%
U0126	MEK1/2	Inhibitor	IC50~0.5 μM	1.1 μM [0.74-1.7]	>80%
SB202474	p38 kinase	Inactive	Non applicable	>10 μM	>50%
SB203580	p38 kinase	Inhibitor	IC50~600 nM	Ineffective	<10%
Lithium	IP3 turnover	Inhibitor	Ki~0.5 μM	Ineffective	<10%
KN62	CAMKII	Inhibitor	Ki~900 nM	Ineffective	<10%
Calphostin C	PKC PKA PKG $p60^{c\text{-}src}$	Inhibitor Inhibitor Inhibitor Inhibitor	IC50~50 nM IC50>50 μM IC50>25 μM IC50>50 μM	>1 μM	~50%
Lavendustin A	EGF receptor $p60^{c\text{-}src}$	Inhibitor Inhibitor	IC50~11 nM IC50~500 nM	>10 μM	<25%
H-89	PKA CAMKII Casein kinase I PKC	Inhibitor Inhibitor Inhibitor Inhibitor	Ki~48 nM Ki~30 μM Ki~38 μM Ki~31.7 μM	>10 μM	<25%

Kinase inhibition activities and potencies were derived from the literature (Chijiwa et al. 1990; Favata et al. 1998; Henry et al. 1998; Inhorn and Majerus 1987; Kobayashi et al. 1989; Lee et al. 1994; Onoda et al. 1989; Tokumitsu et al. 1990). IC50s for neuroprotection are the mean of three separate curves with upper and lower 95% confidence intervals (C.I.) shown. Curves were fit, and confidence intervals were determined using GraphPad Prism software.

Example 4

Evaluation of a MEK1/2 Inhibitor in the Differentiated P19 Assay

U0126 (bis[amino[(2-aminophenyl)thio]methylene] Butanedinitrile) is reported to be highly selective for MEK1/2 (Favata et al. 1998), a result that was confirmed here. The only other kinase found that U0126 inhibits is PKC-γ, but the IC50 for inhibition of this enzyme was 60-fold higher that its published IC50 against wildtype MEK1/2 (Tables II and III below).

The general procedure used to assay for kinase activity was as follows: a kinase reaction mix was prepared in 50 mM Tris-HCl pH=8, 10 mM $MgCl_2$, 0.1 mM Na_3VO_4, 1 mM DTT, 10 μM ATP, 0.25-1 μM biotinylated peptide substrate, 0.2-0.8 μCuries per well ^{33}P-γ-ATP [2000-3000 Ci/mmol]. Assay conditions varied slightly for each protein kinase, for example, insulin receptor kinase requires 10 mM $MnCl_2$ for activity and calmodulin-dependent protein kinase requires calmodulin and 10 mM $CaCl_2$. Reaction mix was dispensed into the wells of a streptavidin-coated Flashplate and 1 μl drug stock in 100% DMSO was added to a 100 μL reaction volume resulting in a final concentration of 1% DMSO in the reaction. Enzyme was diluted in 50 mM Tris-HCl pH=8.0, 0.1 % BSA and added to each well. The reaction was incubated for one hour at 30°C in the presence of compound. After one hour the reaction mix was aspirated from the plate and the plate was washed with PBS containing 100 mM EDTA. The plate was read on a scintillation counter to determine ^{33}P-γ-ATP incorporated into the immobilized peptide. Test compounds were assayed in duplicate at 8 concentrations ranging from 100 μM to 10 pM in one order of magnitude steps. A maximum and minimum signal for the assay was determined on each plate. The IC50 was calculated from the dose response curve of the percent inhibition of the maximum signal in the assay according to the formula [max signal – background/test compound signal-background X (100)] = % inhibition by graphing the percent inhibition against the log

concentration of test compound. Known inhibitor compounds appropriate for the kinase being assayed werealso included on each plate. Results are provided in Figure 3.

Definition and Source of Kinase Enzymes

VEGF-R (vascular endothelial growth factor receptor-2) is a fusion protein containing a polyhistidine tag at the N-terminus followed by amino acids 786-1343 of the rat VEGF-R2 kinase domain. CDK1 (cyclin dependent kinase 1) is isolated from insect cells expressing both the human CDK1 catalytic subunit and its positive regulatory subunit cyclin B. Insulin Receptor Kinase consists of residues 941-1313 of the cytoplasmic domain of the beta-subunit of the human insulin receptor. Protein Kinase A is the catalytic subunit of cAMP-dependent protein kinase-A purified from bovine heart. PKC (protein kinase-C) is the gamma or beta isoform of the human protein produced in insect cells. Casein Kinase 1 is a truncation at amino acid 318 of the C-terminal portion of the rat CK1 delta isoform produced in *E. coli*. Casein Kinase 2 includes the alpha and beta subunits of the human CK2 protein produced in *E. coli*. Calmodulin Kinase (calmodulin-dependent protein kinase 2) is a truncated version of the alpha subunit of the rat protein produced in insect cells. Glycogen Synthase Kinase-3 is the beta isoform of the rabbit enzyme produced in *E. coli*. MAP Kinase is the rat ERK-2 isoform containing a polyhistidine tag at the N-terminus produced in *E. coli* and activated by phosphorylation with MEK1 prior to purification. EGFR (epidermal growth factor receptor) is purified from human A431 cell membranes. The chart below shows selected kinases and their control inhibitors.

As used in Table III below, Compound A (Cmpd A) shall mean the compound have the formula

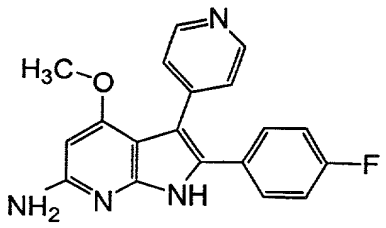

Table II

Selected Kinases and Their Control Inhibitors

Kinase	Control Inhibitor
CDK1	Butyrolactone
EGFR	AG-1478
Protein Kinase A	H89
PKC	Staurosporine
Casein Kinase 1	H89
Casein Kinase 2	
Calmodulin Kinase	Staurosporine
Insulin Kinase	Staurosporine

Table III

Kinase Selectivity of Compound A and U0126

Compound ID	CDK1 (μM)	EGF-R (μM)	PK A (μM)	PKC-γ (μM)
Cmpd A	>100	>100	>100	8.35
U0126	>100	>100	>100	29.5
Compound ID	**Casein Kinase 1 (μM)**	**Casein Kinase 2 (μM)**	**Calmodulin Kinase (μM)**	**Insulin Receptor Kinase (μM)**
Cmpd A	0.116	>100	>100	>100
U0126	>100	>100	>100	ND

IC50 values for kinase inhibition are the mean of at least two separate curves, and were determined using GraphPad curve fitting software.

To determine whether U0126 inhibits the MEK1/2 enzymes in P19 neurons, its ability to block glutamate-induced phosphorylation of the MEK1/2 substrate p42 MAPK (ERK2) was tested. Western blot were first probed using ATRA P19 neuron lysates 9 days post treatment with an antibody specific for the phosphorylated form of p42/44 (ERK1/2) and then stripped and reprobed with antibody that recognized total p42/44 (ERK ½). The data demonstrate that the concentrations of glutamate and glycine that were used to induce toxicity in P19 neurons also induced a rapid, reproducible increase in p42 MAPK phosphorylation in these cells. In the presence of

U0126, phospho-p42 MAPK was reduced, although no change in the amount of total p42 MAPK was evident. In another Western blot experiment, ATRA P19 neuron lysates were probed 9 days post treatment with an antibody specific for the phosphorylated form of p42/44 (ERK ½). The same blot was stripped and reprobed with an antibody that recognized total p42/44 (ERK ½). Glutamate-induced elevation of p42 MAPK phosphorylation was sustained, since it was still clearly increased at 24 h versus controls. These blots are representative of 3 separate experiments with similar results. U0126 blocked the increased levels of phosphorylation at this time point as well. No change in total p42 MAPK was evident.

To ensure that U0126 does not block the NMDA receptor directly, P19 neuron intracellular calcium responses to glutamate and glycine were tested in the presence of 10 μM U0126. Fura-2 imaging traces 9 days post ATRA P19 neurons were treated with 3 mM glutamate, 1 mM glycine in the presence of 10 μM U0126 for 24 hours. U0126 was administered concurrently with glutamate and glycine. Traces are the average ± standard error from four separate experiments for each condition.

The data demonstrated that U0126 did not block this intracellular calcium response. (Figure 4A). It was also demonstrated that U0126 did not inhibit [3H]-MK-801 binding in P19 neurons. No significant inhibition was observed at any concentration of U0126. Data points represent the mean ± standard error from eight experiments. Percent control is defined as described in Figure 1B (Figure 4B). Together, these data further demonstrate that U0126 acts on a signaling pathway downstream of NMDA receptor activation.

The p42/44 MAPK inhibitor, U0126, exhibits delayed neuroprotection

Time-course of efficacy is an extremely relevant parameter for a potential neuroprotective therapeutic agent, since the therapeutic would need to be administered hours to days after an ischemic event and still retain efficacy. The next set of experiments examined whether the MEK1/2 inhibitor, U0126, retains neuroprotective efficacy when added at various time points after glutamate challenge. Assays were performed essentially as described, although the time of administration of the U0126 was delayed relative to the initial excitotoxicity. The data demonstrated that U0126 was maximally neuroprotective up to six hours after glutamate challenge (Figure 5A). However a p38 inhibitor lost efficacy as soon as 15 minutes after glutamate challenge

(Figure 5B). U0126 was maximally neuroprotective even when added several hours after the onset of glutamate challenge. This may be because glutamate mediates a sustained increase in p42 MAPK phosphorylation in P19 neurons, detectable even at 24 hours post glutamate addition. U0126 inhibition of the upstream activating enzyme, MEK, several hours after glutamate challenge may favor phosphatase dephosphorylation of p42 MAPK, and restabilize the p42/44 MAPK signaling pathway within enough time to prevent cell death.

Thus, activation of the p42/44 MAP kinase pathway is necessary for glutamate-induced toxicity in differentiated P19 neurons. Glutamate-induced cell death occurs within 24 hours, is dose-dependent, and is NMDA receptor-mediated. Glutamate induces phosphorylation of p42 MAP kinase, which is blocked by U0126, an inhibitor of its upstream kinase, MEK. U0126 also blocks glutamate toxicity in a dose-dependent manner. It is effective when administered before, or even several hours after the onset of glutamate challenge.

A compound that is able to exert delayed neuroprotection even when added after an ischemic event is an especially sought after property of a potential stroke therapeutic. Many compounds with diverse mechanisms are reported to exhibit post-treatment delayed neuroprotection. Among these are glutamate receptor antagonists (Li et al. 1999b; Takahashi et al. 1998; Turski et al. 1998), antioxidants (Callaway et al. 1999; Pazos et al. 1999; Sakakibara et al. 2000), anticonvulsants (Schwartz-Bloom et al. 1998; Wasterlain et al. 1996; Yang et al. 1998), protease inhibitors (Cheng et al. 1998), kinase inhibitors (Tatlisumak et al. 1998), and magnesium (Heath and Vink 1999). However, this is the first demonstration in a cell culture model of NMDA receptor-mediated excitotoxicity wherein a specific inhibitor of the p42/44 MAP kinase pathway exhibits delayed neuroprotection, and wherein the time window of efficacy extended well after the onset of toxic challenge.

U0126 Neuroprotection is Selective for Glutamate-Induced Toxicity.

To determine whether U0126 is protective against a variety of nonspecific toxic insults, or whether the efficacy of this compound is selective for glutamate-induced toxicity, its effects were tested against a variety of other inducers of P19 neuron death.

Figure 6A shows P19 neuron treatment with various concentrations of A23187 for 24 hours in the presence or absence of 10 μM U0126. Cells were then assayed for

Alamar blue fluorescence. The curve generated through the data points is the average of 3 separate dose response curves. Data points are represented as percent of control cells ± standard error. The EC50 for A23187 toxicity in the absence of U0126 was calculated to be 520 nM [340 nM – 784 nM]. The EC50 for A23187 toxicity in the presence of 10 μM U0126 was calculated to be 833 nM [440 nM – 1.6 μM].

Figure 6B shows that 1 μM staurosporine-induced P19 neuron toxicity could not be protected by 10 μM U0126, as measured by Alamar blue fluorescence at 24 hours after addition. Cells that received vehicle rather than staurosporine exhibited control levels of Alamar blue fluorescence. However no concentration of U0126 brought fluorescence back to control levels in staurosporine-treated cells.

Figure 6C demonstrated Alamar blue fluorescence assayed on P19 neurons treated with vehicle or with 10 μM U0126 in the absence of any inducers of toxicity. U0126 alone did not affect these control levels of fluorescence. The data demonstrate that U0126 was not protective against staurosporine or A23187-induced death (Figures 6A,6B). Additionally, U0126 did not affect the basal viability of P19 neurons (Figure 6C).

Example 5
Drug Screening Using Differentiated P19 Cell Assay

Commercially available chemical libraries (BioFocus PLC, UK) were screened using the methods described herein. The stock concentration of the compounds was about 400 μM in DMSO. The concentration of compounds used in the primary screen was 1 μM. A positive compound was assigned as one that demonstrated 70% or greater neuroprotection. Dose-response testing was carried out in 96 well plates where column 1 was vehicle control, column 2 received 3 mM glutamate and 1 mM glycine, and column 3 received 3 mM glutamate, 1 mM glycine, and 10 μM U0126. Columns 4-11 received compounds at the following final concentrations (μM): 3, 1.2, 0.48, 0.192, 0.077, 0.031, 0.012 and 0.005. Each row contained a different compound for confirmation. Only rows B-G received compounds, and rows A and H remained untreated. Data are expressed as % neuroprotection = ((compound-glutamate average)/(U0126-glutamate average) X 100).

Compounds of two genuses, 4-pyrimidinamines and 2-pyridinamines, were found to display neuroprotective properties as data here show. Only the 2-pyridinamines are the subject of this invention, although limited data for 4-pyrimidinamines are presented as well. The results of this biological testing are summarized in the following tables. "% Inh" indicates the percentage of control cells surviving after 24 hours, and represents the neuroprotective effect of the compounds screened at 1 micromolar concentration. IC50 relate to data from dose response experiments. IC50 values listed as >1 indicate no observed maximum within the highest dose tested (3 μM), yet indicate biological activity. ND refers to compounds not tested in dose-response experiments.

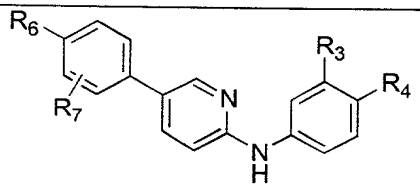

Table IV

N,5-diphenyl-2-pyridinamine derivatives

Cmpd	R_6	R_7	R_4	R_3	IC_{50} (μM)	% Inh
1	OH	H	morpholinyl	H	1.08	84
2	OH	H	OCH_3	H	0.56	94
3	OCF_3	H	OCH_3	H	0.51	94
4	OCF_3	H	fused to form 2,3-dihydro-1,4-benzodioxinyl		0.38	86
5	morpholinyl	H	fused to form 2,3-dihydro-1,4-benzodioxinyl		0.284	80
6	morpholinyl	H	pentoxy	H	0.22	83
7	$N(CH_3)_2$	H	pentoxy	H	0.24	88
8	$N(CH_3)_2$	H	methoxy	H	0.2	83
9	OH	H	pentoxy	H	0.56	84
10	$(CH_2)_2COOH$	H	pentoxy	H	0.23	105
11	H	2-methoxy	fused to form 2,3-dihydro-1,4-benzodioxinyl		0.87	83
12	H	3-ethoxy	methoxy	3,5-dimethoxy	0.047	87
13	fused to form 1,3-benzodioxolyl		pentoxy	H	0.26	98
14	H	2-methoxy	pentoxy	H	0.22	90
25	fused to form 2-naphthyl		morpholinyl	H	0.084	100
28	H	2-phenoxy	morpholinyl	H	>1	83
29	Cl	H	morpholinyl	H	>1	82

30	fused to form 1,3-benzodioxolyl		morpholinyl	H	>1	84
31	F	3-Cl	morpholinyl	H	>1	83
32	H	2-methoxy	morpholinyl	H	>1	100
33	H	3-OCF_3	morpholinyl	H	>1	89
34	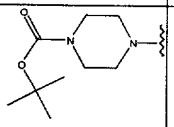	H	methoxy	H	>1	88
35	H	2-methoxy	methoxy	H	>1	82
36	H	3-amine	pentoxy	H	>1	98
68	-OCF_3	H	fused to form 2,3-dihydro-1,4-benzodioxiny		0.38	86
17	-OCF_3	H	morpholinyl	H	ND	74
18	H	3-OCF_3	methoxy	H	ND	74
38	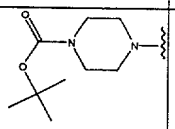	H	H	-$N(CH_3)_2$	ND	89
40	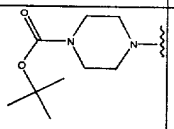	H	methoxy	3,5-dimethoxy	ND	77
69	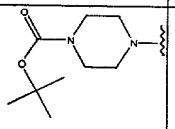	H	fused to form 2,3-dihydro-1,4-benzodioxinyl		ND	99
70	OH	H	fused to form 2,3-dihydro-1,4-benzodioxinyl		ND	93
71	H	2-methoxy	methoxy	3,5-dimethoxy	ND	77
72	H	2-methoxy	fused to form 2,3-dihydro-1,4-benzodioxinyl		0.87	83
73	H	3-ethoxy	fused to form 2,3-dihydro-1,4-benzodioxinyl		ND	76
74	H	3-$N(CH_3)_2$	methoxy	3,5-dimethoxy	ND	95
75	H	3-$N(CH_3)_2$	pentoxy	H	ND	88

76	H	3-$N(CH_3)_2$	fused to form 2,3-dihydro-1,4-benzodioxinyl		ND	95
77	morpholinyl	H	fused to form 9 ethyl 9H-carbazole		ND	82
78	Phenyl	H	morpholinyl	H	0.47	109
79	methoxy	3-methoxy	morpholinyl	H	0.46	110
80	CH_3	3-CH_3	morpholinyl	H	0.75	94
81	fused to form 2-naphthyl		fused to form 2,3-dihydro-1,4-benzodioxinyl		0.47	107
82	H	H	methoxy	H	ND	72
83	morpholinyl	H	methoxy	H	ND	71
84	CH_3	3-CH_3	methoxy	3,5-dimethoxy	0.49	85
85	CH_3	3-CH_3	fused to form 2,3-dihydro-1,4-benzodioxinyl		>1	86
86	CH_3	3-CH_3	methoxy	H	>1	80
87	CH_3	3-CH_3	H	$N(CH_3)_2$	>1	84
94	COOH	H	pentoxy	H	0.78	104
95	H	3-$N(CH_3)_2$	morpholinyl	H	>1	101
96	H	3-COOH	pentoxy	H	0.5	106

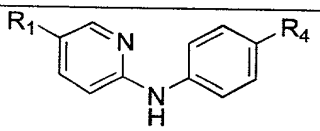

Table V

N-phenyl-2-pyridinamine derivatives

Cmpd	R_1	R_4	IC_{50} (μM)	% Inh
19	2,4-dimethoxy-5-pyrimidinyl	pentoxy	0.99	99
20	3-thienyl	morpholinyl	0.68	105
21	3,5-bis(trifluoromethyl) phenyl	morpholinyl	0.21	95
22	2,7a-dihydrobenzo[*b*] thien-2-yl	morpholinyl	0.09	98
23	3a,7a-dihydro-2-benzofuranyl	morpholinyl	0.92	96
24	3,4,5-trimethoxyphenyl	morpholinyl	1.76	94
26	2,3-dichlorophenyl	morpholinyl	>1	107
37	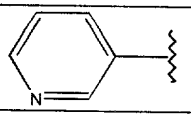	pentoxy	ND	84

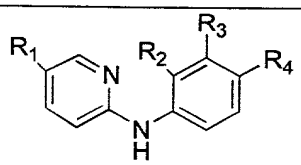

Table VI

5-R1-N-phenyl-2-pyridinamine derivatives

Cmpd	R_1	R_2	R_3	R_4	IC_{50} (μM)	% Inh
88	-$(CH)_2$Ph	H	fused to form 2,3-dihydro-1,4-benzodioxinyl		0.23	85
89	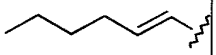	H	fused to form 2,3-dihydro-1,4-benzodioxinyl		1.0	83
90	-$(CH)_2$Ph	CH_3	H	methoxy	ND	73
91	furanyl	H	methoxy	3,5-dimethoxy	0.5	90
92	furanyl	H	fused to form 2,3-dihydro-1,4-benzodioxinyl		ND	74
93	furanyl	H	methoxy	H	ND	76

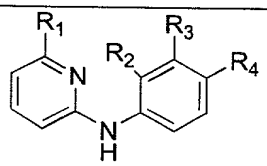

Table VII

6-R1-N-phenyl-2-pyridinamine derivatives

Cmpd	R_1	R_2	R_3	R_4	IC_{50} (μM)	% Inh
94	4-(OH)Ph-	H	H	methoxy	ND	86
95	(4-thienyl)-	H	H	methoxy	0.54	110
96	3-($(CF_3)O$)Ph-	H	H	methoxy	ND	76
97	(2-naphthyl)-	H	H	methoxy	ND	71
98	4-($(CH_3)_2N$)Ph-	H	H	methoxy	ND	71
99	3-(NH_2)Ph-	H	fused to form 9 ethyl 9H-carbazole		0.33	105
100	3-(NH_2)Ph-	H	H	methoxy	ND	79
101	2-(PhO)Ph-	H	H	methoxy	ND	78
102	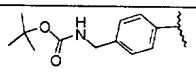	H	H	methoxy	0.94	103
103	4-(Cl)Ph-	H	H	methoxy	ND	75
104	3-($(CH_3)_2N$)Ph-	H	fused to form 9 ethyl 9H-carbazole		0.09	89
105	3-($(CH_3)_2N$)Ph-	H	H	methoxy	0.4	98
106	4-morpholinyl-phenyl-	H	3,5-dimethoxy	methoxy	0.66	84
107	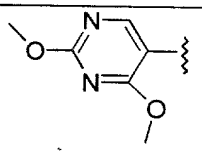	H	3,5-dimethoxy	methoxy	ND	71
108	4-($(CF_3)O$)Ph-	CH_3	methoxy	methoxy	>1	84
109	4-($(CH_3)_2N$)Ph-	CH_3	methoxy	methoxy	ND	79
110	(2-benzofuranyl)-	H	3,5-dimethoxy	methoxy	0.14	91
111	(2-benzofuranyl)-	CH_3	methoxy	methoxy	>1	90
112	3,4,5-	H	3,5-	methoxy	0.9	90

	$((CH_3)O)_3Ph$-		dimethoxy			
113	3-$((CH_3)_2N)Ph$-	H	3,5-dimethoxy	methoxy	0.54	91
114	3-$(CH_3CH_2O)Ph$-	H	3,5-dimethoxy	methoxy	0.14	96
115	3-$(CH_3CH_2O)Ph$-	CH_3	methoxy	methoxy	1.1	83
116	(benzo[b] thien-2-yl)-	CH_3	methoxy	methoxy	1.5	83
117	4-(OH)Ph-	H	3,5-dimethoxy	methoxy	ND	78
118	3-$((CF_3)O)Ph$-	H	3,5-dimethoxy	methoxy	0.05	91
119	4-(OH)Ph-	CH_3	methoxy	methoxy	ND	73
120	(1,3-benzodioxol-5-yl)-	H	3,5-dimethoxy	methoxy	0.05	97
121	4-(Ph)Ph-	H	3,5-dimethoxy	methoxy	0.65	96
122	Ph-	H	3,5-dimethoxy	methoxy	0.007	84
123	Ph-	H	H	methoxy	0.65	90
124	3,4-$(CH_3O)_2Ph$-	H	3,5-dimethoxy	methoxy	0.23	86
125	3,4-$(CH_3O)_2Ph$-	CH_3	methoxy	methoxy	0.23	76
126	3,4-$(CH_3)_2Ph$-	H	3,5-dimethoxy	methoxy	0.08	90
127	3,4-$(CH_3)_2Ph$-	CH_3	methoxy	methoxy	0.19	86
128	3,4-$(CH_3)_2Ph$-	H	H	methoxy	1.54	84
129	3,4-$(CH_3O)_2Ph$-	H	fused to form 9 ethyl 9H-carbazole		0.34	92

130	3,4-$(CH_3O)_2$Ph-	H	H	methoxy	0.85	96
131	(2-furanyl)-	H	H	methoxy	0.24	95
132	(2-furanyl)-	H	fused to form 9 ethyl 9H-carbazole		>1	105
134	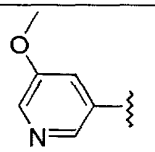	H	fused to form 9 ethyl 9H-carbazole		1.59	92
135	(2-naphthyl)-	H	3,5-dimethoxy	methoxy	0.21	86
136	(2-naphthyl)-	CH_3	methoxy	methoxy	>1	86
137	3,5-$(CF_3)_2$Ph-	H	3,5-dimethoxy	methoxy	0.59	82
138	2-(PhO)Ph-	H	3,5-dimethoxy	methoxy	0.23	90
139	(1,3-benzo dioxol-5-yl)-	H	fused to form 9 ethyl 9H-carbazole		ND	72
140	(1,3-benzo dioxol-5-yl)-	H	H	-O(Ph)	ND	79
141	4-(Cl)Ph-	H	3,5-dimethoxy	methoxy	ND	76
142	3-(Cl),4-(Fl)Ph-	H	3,5-dimethoxy	methoxy	ND	94
143	3-(Cl),4-(Fl)Ph-	CH_3	methoxy	methoxy	0.8	85
144	$Ph(CH)_2$-	H	3,5-dimethoxy	methoxy	0.03	110
145	$Ph(CH)_2$-	CH_3	methoxy	methoxy	0.28	96
146	3,4-$(Cl)_2$Ph-	H	3,5-dimethoxy	methoxy	0.32	99

Example 6

2-Pyridinamine and 4-Pyrimidinamine Derivatives

Do Not Inhibit MEK Activity in P19 Neurons.

The commercially available 2-pyridinamine and 4-pyrimidinamine compounds tested here did not inhibit MEK1/2 kinase activity in P19 neurons since they did not inhibit glutamate-induced p44/42 MAP kinase phosphorylation in these cells. However U0126 did inhibit this activity as expected (Figure 8). MEK activity in P19 neurons was induced by addition of 3 mM glutamate and 1 mM glycine, and measured by assaying for phosphorylation of the MEK substrate, p44/42 MAP kinase. Cells were treated with the compounds described herein or with U0126 in the presence or absence of glutamate/glycine, and harvested 5 minutes after treatment, for subsequent Western blot analysis. The data demonstrate that U0126 effectively inhibited phosphorylation of MEK substrate as expected, but that the 2-pyridinamine and 4-pyrimidinamine compounds did not. Therefore, the 2-pyridinamine and 4-pyrimidinamines are not MEK inhibitors.

The 2-pyridinamine and 4-pyrimidinamines were maximally neuroprotective at least two hours after the onset of excitotoxicity. Compounds were administered at a concentration of 1 μM either 15 minutes before or 2 hours after glutamate/glycine addition. U0126 was tested as a positive control. Similar to U0126, the 2-pyridinamine and 4-pyrimidinamine compounds retained maximal neuroprotective efficacy at both time points despite being active at a different target.

Example 7

In Vivo Model of Neuroprotection:

Middle Cerebral Artery Occlusion Protocol

Spontaneous hypertensive (SHR) male rats, approximately 90-100 days old (~250-300g), are weighed and then anesthetized with ketamine (100mg/ml)/ xylazine (20mg/ml) cocktail (1.2ml/kg; i.p.) followed by subcutaneous administration of a long-acting antibiotic (e.g., combiotic). The level of anesthetic are assessed by corneal reflex (air puff to eye) and leg jerk in response to tail or foot pinch. Once the rat is anesthetized, it is placed on a small animal surgical board and restrained during the surgical procedure. The rat's body temperature is monitored with a rectal probe and maintained at 37°C with a homeostatic heating pad. Areas of incision are shaved and swabbed with betadine. The surgical area is aseptic. All surgical instruments are

sterilized in an autoclave and/or in a glass bead dry instrument sterilizer, then rinsed with sterile saline or alcohol before use.

(1) Femoral Artery Catheter. An indwelling catheter is placed in the femoral artery for periodic blood sampling and measurement of arterial blood pressure. An incision is made over the area of the femoral artery. Tissue is blunt dissected to isolate the artery. The distal end of the artery is ligated with sterile suture and a loose ligature placed around the proximal end for securing the catheter in place. A small incision is made in the artery for insertion of the catheter. The bevel-tipped end of PE50 tubing is inserted 5mm into the artery and then secured in place by sterile suture. The PE tubing is attached to a 1cc syringe filled with heparinized saline that is used minimally to keep the artery patent. Arterial blood is sampled three times: 10 minutes before ischemia, 2h after the onset of ischemia and 15 minutes post-reperfusion. All blood samples are taken in 100-300µl volumes to determine pH, PaO_2, $PaCO_2$, hematocrit and glucose. The maximum amount of blood withdrawn throughout the experiment does not exceed 1ml per animal. When blood sampling is not occurring, a blood pressure transducer is attached to the catheter to measure mean arterial pressure. At the end of the surgical procedure, the catheter is removed, the artery tied off and the incision area sutured shut.

(2) Tandem CCA-MCA Occlusion Model of Focal Cerebral Ischemia. Male spontaneously hypertensive Wistar rats (SHRs) are prepared for reversible focal cerebral ischemia by unilateral occlusion of both the common carotid artery (CCA) and the middle cerebral artery (MCA), using a modification of the technique described by Brint and co-workers (J. Cereb Blood Flow Metab 8:474-485, 1988). The left CCA is isolated through an incision in the ventral surface of the neck. For isolation of the ipsilateral MCA, a second incision is made between the lateral canthus of the left eye and the corresponding external auditory canal to bare the underlying skull. The MCA is exposed through a 5mm burrhole drilled 2-3mm rostral to the fusion of the zygomatic arch and the squamosal bone under direct visualization with a Zeiss operating microscope. The dura is opened with a sterile 26g needle and a platinum wire (0.1mm diameter) is inserted beneath the MCA just superior to the inferior cortical vein. The MCA is temporarily occluded by elevation and compression of the vessel across the platinum wire, as described by Aronowski and colleagues (Stroke, 25:2235-2240, 1994). Concurrently, the CCA is occluded with an aneurysm clip. The duration of occlusion of the CCA and the MCA is 2h. At the end of this period, the wire and the

clip are carefully removed to allow reperfusion of the vessels and the incision area sutured shut. The rat is placed in an isolation cage to recover before returning to his home cage. The rat is closely monitored for 2-4h post surgery to ensure uneventful recovery from the anesthesia and surgical procedure. Following recovery from anesthesia, the rat is housed according to the established protocol as per LAM guidelines until required for the experimental analysis.

(3) Test compounds are administered by any suitable route: intravenous, subcutaneous, or intraperitoneal. Dose and time of compound administration is based on *in vitro* assay results or literature references.

(4) Two outcome measures are used to assess compound efficacy: (a) behavioral performance on several CNS paradigms such as the Morris Water Maze, spontaneous motor activity, radial arm maze, and CNS general behavior profile; and (b) histological examination of the size of the cerebral cortical infarct. Twenty-four hours post-ischemia, rats are tested in a behavioral paradigm and then subsequently euthanized for brain histology. Rats are deeply anesthetized with an intraperitoneal injection of sodium pentobarbital (100 mg/kg, i.p). Depth of anesthesia is checked by lack of corneal reflex and tail pinch. Rats are euthanized by transcardial perfusion with approximately 50 ml heparinized physiological saline. After perfusion, the brain is removed, blocked and sectioned into 1mm slabs. Each slab is placed in TTC solution, a cell viability dye, for 15 min. The stained slabs are visualized with a Nikon SMZ-U dissecting microscope and image analysis of the affected brain areas are quantified using ImagePro 2.1 software. Infarct volume is expressed as % of contralateral hemisphere. Statistical comparisons are made across treatment groups (one-way ANOVA).

Example 8

In Vivo Study: Transient Model of Cerebral Ischemia

Male Wistar rats (Iffa Crédo, France), weighing 250-300 g, are housed 2 per cage under a light-dark cycle of 12 hr - 12 hr (light on at 7:00 a.m., off at 7:00 p.m.) at a room temperature of 21±2°C, with 50±15% humidity, for a minimum of 5 days before the experiments. During this time, the rats have free access to commercial rat chow (Trouw Nutrition France, Vigny, France, ref. 811002) and tap water.

Animals are anaesthetized with 5% halothane in air for induction, then 1-2% halothane during surgery. The rat's body temperature is maintained at 37°C with a heating pad. A 2cm incision is made at the center of the neck and the right common carotid artery (CCA), external carotid artery (ECA) and internal carotid artery (ICA) are exposed under an operating microscope. The ICA is further dissected to identify the pterygopalatine artery (PA) branch and the intracranial ICA branch. The CCA is ligated. A 3-0 silk suture is tied at the origin of the ECA and ligated. A catheter (id = 0.58 mm) is introduced into the CCA through a small puncture and advanced to the intracranial branch of the ICA. A 4-0 surgical nylon suture is introduced into the catheter. A length of approximately 19mm of nylon suture is gently advanced from the CCA into the lumen of the ICA until the suture blocks the origin of the MCA. The suture is sealed into the catheter by heat, leaving 1cm of catheter protruding so the suture can be withdrawn to allow reperfusion. The incision is closed using skin clips. Anaesthesia is then terminated and the animals are placed under heat lamps until recovery from anaesthesia. The rats awake 10-15 min later. After 2 hr of ischemia, reperfusion is performed by withdrawal of the suture until the tip clears the ICA lumen. Vehicle or test compound is administered intraperitoneally (*i.p.*) at 1hr post ischemia onset.

24 h after the onset of occlusion, the rats are killed by decapitation. The brains are immediately removed, frozen in isopentane and stored at -20°C. The brains are then cut in 20 µm thick sections in a cryocut. Every 20th slice is used to measure infarct area. The sections are stained with cresyl violet and the areas of infarct in the striatum and cortex are determined by planimetry using an image analysis software (Image, NIH) after digitalization of the section images. Results are expressed as volume of cortex and striatum (mm^3) from the frontal to the occipital cortex. Data are analysed by variance analysis (ANOVA 1-way) followed by Dunnett's t-test.

While the foregoing specification teaches the principles of the present invention, with examples provided for the purpose of illustration, it will be understood that the practice of the invention encompasses all of the usual variations, adaptations and/or modifications as come within the scope of the following claims and their equivalents.

References

Ahn, N., et al. (1991) *J. Biol. Chem.* 266:4220-4227.

Alessandrini, A., et al. (1999) *Proc Natl Acad Sci U S A* 96:12866-9.

Anderson, N., et al. (1990) *Nature* 343:651-653.

Bading, H., Greenberg, M. E. (1991) *Science* 253:912-914.

Callaway, J., et al. (1999) *Stroke* 12:2704-2712.

Canzoniero, L., et al. J. (1996) *J. Neurosci. Res.* 45:226-236.

Cheng, Y., et al. (1998) *J. Clin. Invest.* 101:1992-1999.

Chijiwa, T., et al. (1990) *J. Biol. Chem.* 265:5267-5272.

Courtney, M., et al. (1990) *J Neurosci.* 10:3873-3879.

Crews, C., Alessandrini, A., Erikson, R. (1992). *Science* 258:478-480.

Desdouits-Magnen, J., et al. (1998) *J. Neurochem.* 70:524-530.

Enslen, H., et al. (1996) *Proc Natl Acad Sci USA* 93:10803-10808.

Favata, M. F., et al., (1998) *J. Biol. Chem.* 273:18623-18632.

Fiore, R. S., et al. (1993) *J Neurochem* 61:1626-1633.

Grobin, A. C., (1999). *Brain Research* 827:1-11.

Heath, D., Vink, R. (1999). *J. Neurosurg.* 90:504-509.

Henry, J., et al. (1998) *J. Med. Chem.* 41:4196-4198.

Hu, B., Wieloch, T. (1994) *J. Neurochem.* 62:1357-1367.

Inhorn, R., Majerus, P. (1987) *J. Biol. Chem.* 262:15946-15952.

Ishii, T., et al. (1993) *J. Biol. Chem.* 268:2836-2843.

Jaiswal, R., et al. (1994) *Mol. Cell. Biol.* 14:6944-6953.

Jones-Velleneuve, et al. (1982) *J. Cell Biol.* 94:253-262.

Jones-Villeneuve, et al. (1983) *Mol. Cell Biol.* 3:2271-2279.

Jovanovic, J., et al. (1996) *Proc. Natl. Acad. Sci. USA* 93:3679-3683.

Kindy, M. (1993) *J Cereb Blood Flow Metab* 13:372-377.

Kobayashi, E., et al. (1989) *Biochem. Biophys. Res. Commun.* 159:548-553.

Kurino, M., et al. (1995) *J Neurochem* 65:1282-1289.

Lander, H., et al. (1996) *J. Biol. Chem.* 271:19705-19709.

Laurie, D., et al. (1995) *Brain Res. Mol. Brain Res.* 32:94-108.

Lee, J., et al. (1994) *Nature* 372:739-746.

Lev, S., et al. (1995) *Nature* 376:737-745.

Li, B., et al. (1999a) *Eur. J. Biochem.* 262:211-217.

Li, M., et al. (1999b) *Brain Res.* 1999:44-52.

McBurney, M. W., et al. (1982) *Dev. Biol.* 89:503-508.

Meldrum, B., Garthwaite, J. (1990) *Trends Pharmacol Sci* 11:379-387.

Monyer, H., et al. (1994) *Neuron* 12:529-540.

Monyer, H., et al. (1992) *Science* 256:1217-1221.

Moodie, S., et al. (1993) *Science* 260:1658-1661.

Morley, P., et al. (1995) *J. Neurochem.* 65:1093-1099.

Murray, B., et al. (1998) *Proc. Natl. Acad. Sci. USA* 95:11975-11980.

Onoda, T., et al. (1989) *J. Nat. Prod.* 52:1252-1257.

Papin, C., et al. (1995) *Oncogene* 10:1647-1651.

Park, C., et al. (1988) *Ann. Neurol.* 24:543-551.

Pazos, A., et al. (1999) *Brain Res.* 846:186-195.

Pleasure, S., Lee, V.-Y. (1993) *Journal of Neurosci. Res.* 35:585-602.

Pleasure, S., et al. (1992) *J. Neurosci.* 12:1802-1815.

Ray, W. J., Gottlieb, D. I. (1993) *Biochem. Biophys. Res. Comm.* 197:1475-1482.

Rootwelt, T., et al. (1998) *J. Neurochem.* 71:1544-1553.

Rosen, L., et al. (1994) *Neuron* 12:1207-1221.

Sakagami, H., Kondo, H. (1993) *Brain Res Mol Brain Res* 19:215-218.

Sakakibara, Y., et al. (2000) *Neurosci Lett* 281:111-114.

Sattler, R., et al. (1999) *Science* 284:1845-1848.

Schneggenburger, R., et al. (1993) *Neuron* 11:133-143.

Schwartz-Bloom, R., et al. (1998) *J Cereb Blood Flow Metab* 18:548-558.

Sola, C., et al. (1999) *J Neurosci. Res.* 57:651-652.

Stanciu, M., et al. (2000) *J. Biol. Chem.* 275:12200-12206.

Standaert, D., et al. (1994) *J. Comp. Neurol.* 343:1-16.

Takahashi, M., et al. (1998) *J. Pharmacol. Exp. Ther.* 287:559-566.

Tatlisumak, T., et al. (1998) *Stroke* 29:1952-1958.

Tokumitsu, H., et al. (1990) *J. Biol. Chem.* 265:4315-4320.

Turetsky, D. M., et al. (1993) *J. Neurobiol.* 24:1157-1169.

Turski, L., et al. (1998) *Proc. Natl. Acad. Sci. USA* 95:10960-10965.

Tymianski, M., et al. (1993) *J. Neurosci.* 13:2085-2104.

Vanhoutte, P., et al. (1999) *Mol. Cell. Biol.* 19:136-146.

Wasterlain, C., et al. (1996) *Stroke* 27:1236-1240.

Xia, Z., et al. (1995) *Science* 270:1326-1331.

Xia, Z., et al. (1996) *J. Neurosci.* 16:5425-5436.

Yang, D. D., et al. (1997) *Nature* 389:865-870.

Yang, Y., et al. (1998) *Brain Res.* 804:169-176.

Zheng, C., et al. (1993) *J. Biol. Chem.* 268:23933-23939.

5